

## 基础研究

# 大鼠脊髓背角胶状质神经元的去极化反跳及调控机制

李凌超<sup>1</sup>, 张达颖<sup>1</sup>, 彭斯聪<sup>2</sup>, 吴 静<sup>2</sup>, 蒋昌宇<sup>4</sup>, 柳 涛<sup>2,3,4</sup>南昌大学第一附属医院<sup>1</sup>疼痛科, <sup>2</sup>儿科, <sup>3</sup>医学科研中心, 江西 南昌 330006; <sup>4</sup>深圳市南山医院韩济生院士疼痛医学工作站, 广东 深圳 518052

**摘要:**目的 研究大鼠脊髓背角胶状质(SG)神经元的去极化反跳及调控机制,以期对去极化反跳相关疾病的临床治疗提供参考。**方法**选取3~5周龄SD大鼠,制作离体脊髓纵切片,应用全细胞膜片钳技术记录SG神经元的电生理学特点及接受超极化刺激后的反应,并观察超极化激活环核苷酸门控阳离子(HCN)通道阻断剂和T型钙(Cav3)通道阻断剂对去极化反跳的作用。**结果**共记录了63个SG神经元的电活动,其中23个无去极化反跳,19个为去极化反跳无放电,21个为去极化反跳伴放电。无去极化反跳组SG神经元的动作电位阈值( $-28.7 \pm 1.6$  mV)明显高于去极化反跳伴放电组( $-36.0 \pm 2.0$  mV)( $P < 0.05$ )。HCN通道阻断剂氯化铯和ZD7288可显著延长去极化反跳伴放电的潜伏期,分别从 $45.9 \pm 11.6$  ms增加到 $121.6 \pm 51.3$  ms( $P < 0.05$ )和从 $36.2 \pm 10.3$  ms增加到 $73.6 \pm 13.6$  ms( $P < 0.05$ );ZD7288也能显著延长去极化反跳不伴放电的潜伏期,从 $71.9 \pm 35.1$  ms增加到 $267.0 \pm 68.8$  ms( $P < 0.05$ ),而T型钙通道阻断剂氯化镍和米贝地尔可显著降低去极化反跳伴放电的振幅,分别从 $19.9 \pm 6.3$  mV降到 $9.5 \pm 4.5$  mV( $P < 0.05$ )和从 $26.1 \pm 9.4$  mV降到 $15.5 \pm 5.0$  mV( $P < 0.05$ ),米贝地尔同样能显著降低去极化反跳不伴放电的振幅,从 $14.3 \pm 3.0$  mV降低至 $7.9 \pm 2.0$  mV( $P < 0.05$ )。**结论**近2/3的SG神经元有去极化反跳,其潜伏期和振幅分别受HCN通道和T型钙通道调控。

**关键词:**去极化反跳;脊髓背角胶状质神经元;超极化激活环核苷酸门控阳离子通道;T型钙通道;全细胞膜片钳记录

## Rebound depolarization of substantia gelatinosa neurons and its modulatory mechanisms in rat spinal dorsal horn

LI Lingchao<sup>1</sup>, ZHANG Daying<sup>1</sup>, PENG Sicong<sup>2</sup>, WU Jing<sup>2</sup>, JIANG Changyu<sup>4</sup>, LIU Tao<sup>2,3,4</sup><sup>1</sup>Department of Pain Clinic, <sup>2</sup>Department of Pediatrics, <sup>3</sup>Center for Experimental Medicine, First Affiliated Hospital of Nanchang University, Nanchang, 330006, China; <sup>4</sup>Jisheng Han Academician Workstation for Pain Medicine, Nanshan Hospital, Shenzhen 518052, China

**Abstract: Objective** To investigate the rebound depolarization of substantia gelatinosa (SG) neurons in rat spinal dorsal horn and explore its modulatory mechanisms to provide better insights into rebound depolarization-related diseases. **Methods** Parasagittal slices of the spinal cord were prepared from 3- to 5-week-old Sprague-Dawley rats. The electrophysiologic characteristics and responses to hyperpolarization stimulation were recorded using whole-cell patch-clamp technique. The effects of hyperpolarization-activated cyclic nucleotide gated cation (HCN) channel blockers and T-type calcium channel blockers on rebound depolarization of the neurons were studied. **Results** A total of 63 SG neurons were recorded. Among them, 23 neurons showed no rebound depolarization, 19 neurons showed rebound depolarization without spikes, and 21 neurons showed rebound depolarization with spikes. The action potential thresholds of the neurons without rebound depolarization were significantly higher than those of the neurons with rebound depolarization and spikes ( $-28.7 \pm 1.6$  mV vs  $-36.0 \pm 2.0$  mV,  $P < 0.05$ ). The two HCN channel blockers CsCl and ZD7288 significantly delayed the latency of rebound depolarization with spike from  $45.9 \pm 11.6$  ms to  $121.6 \pm 51.3$  ms ( $P < 0.05$ ) and from  $36.2 \pm 10.3$  ms to  $73.6 \pm 13.6$  ms ( $P < 0.05$ ), respectively. ZD7288 also significantly prolonged the latency of rebound depolarization without spike from  $71.9 \pm 35.1$  ms to  $267.0 \pm 68.8$  ms ( $P < 0.05$ ). The T-type calcium channel blockers NiCl<sub>2</sub> and mibepradil strongly decreased the amplitude of rebound depolarization with spike from  $19.9 \pm 6.3$  mV to  $9.5 \pm 4.5$  mV ( $P < 0.05$ ) and from  $26.1 \pm 9.4$  mV to  $15.5 \pm 5.0$  mV ( $P < 0.05$ ), respectively. Mibepradil also significantly decreased the amplitude of rebound depolarization without spike from  $14.3 \pm 3.0$  mV to  $7.9 \pm 2.0$  mV ( $P < 0.05$ ). **Conclusion** Nearly two-thirds of the SG neurons have rebound depolarizations modulated by HCN channel and T-type calcium channel.

收稿日期:2016-08-19

基金项目:国家自然科学基金(81560198, 31660289);南昌大学研究生创新基金(cx2015166)

Supported by National Natural Science Foundation of China (81560198, 31660289).

作者简介:李凌超,在读硕士研究生,主治医师,E-mail: 19893395@qq.com;张达颖,主任医师,博士生导师,E-mail: zdy@medmail.com.cn。李凌超、张达颖共同为第一作者

通信作者:柳涛,副主任医师,硕士生导师,E-mail: liutaomm@hotmail.com

**Keywords:** rebound depolarization; spinal dorsal substantia gelatinosa neurons; hyperpolarization-activated cyclic nucleotide gated cation channel; T-type calcium channel; whole-cell patch-clamp recording

位于脊髓背角Ⅱ层的胶状质(SG)区,是从外周向中枢传递伤害性信息的中继站,研究SG神经元的基本电生理特性及其离子基础,对探讨伤害性信息的产生、传递及调控机制具有非常重要的意义<sup>[1]</sup>。研究表明,许多区域的神经元在接受抑制性的信号输入(超极化刺激)后,可将其转化为兴奋性的信号输出(去极化反跳)<sup>[2]</sup>。去极化反跳通常在超极化刺激结束时出现,表现为神经元的一个瞬时去极化反应,在不同脑区具有不同的生理功能。例如,脑干听觉中枢的上橄榄旁核神经元的去极化反跳可编码声音的终止信号<sup>[3]</sup>;小脑深部核团的去极化反跳参与运动学习过程<sup>[4]</sup>。调控去极化反跳的离子通道主要是T型钙通道(Cav3),有时包括超极化激活环核苷酸门控阳离子(HCN)通道<sup>[5]</sup>。脊髓背角I~IV层神经元中均发现有Cav3 mRNA的表达<sup>[6]</sup>,有研究探讨了IV~VI层神经元去极化反跳的特点<sup>[7]</sup>,但Ⅱ层中具有去极化反跳SG神经元的特点及调控机制目前尚无报道。因此,本研究应用红外可视法全细胞膜片钳技术,观察离体脊髓薄片中表达去极化反跳的SG神经元的基本电生理特点及离子基础,为进一步揭示SG神经元兴奋性调控机制和寻求临床疼痛治疗新靶点提供实验依据。

## 1 材料和方法

### 1.1 实验动物和脊髓薄片制备

本研究的动物实验严格按照《南昌大学实验动物管理办法》和《南昌大学动物实验伦理审查》原则进行。健康3~5周龄Sprague Dawley(SD)大鼠,雌雄不拘,体质量80~150 g(江西中医药大学动物中心提供)。动物以乌拉坦(1.2 g/kg)腹腔注射深部麻醉后,用0~4 °C通有混合气(95% O<sub>2</sub>+5% CO<sub>2</sub>)的解剖液100 mL行心脏灌流,灌流同时迅速分离脊柱旁肌肉、离断两侧肋骨,取出脊柱并完全浸入解剖液中;以腹侧入路切除椎板,以腰骶膨大部为中心取出脊髓(腰1~骶3),在实体解剖显微镜下,剥离脊髓表面的硬脊膜、软脊膜及附着神经根后,放置于3%的琼脂块切槽中,用振动切片机(VT1000S, Leica)切取300 μm厚的脊髓纵切片,并移至通有混合气的人工脑脊液(artificial cerebrospinal fluid, ACSF)中,32 °C孵育30 min以上。

### 1.2 溶液和试剂

解剖液组成成分为(mmol/L): sucrose 240, NaHCO<sub>3</sub> 25, KCl 2.5, NaH<sub>2</sub>PO<sub>4</sub>·2H<sub>2</sub>O 1.25, CaCl<sub>2</sub>·2H<sub>2</sub>O 0.5, MgCl<sub>2</sub>·6H<sub>2</sub>O 3.5, ascorbic acid 0.4, sodium pyruvate 2(pH=7.4, 310 mOsm); ACSF组成成分为(mmol/L): NaCl 117, KCl 3.6, NaH<sub>2</sub>PO<sub>4</sub>·2H<sub>2</sub>O 1.2, CaCl<sub>2</sub>·2H<sub>2</sub>O 2.5, MgCl<sub>2</sub>·6H<sub>2</sub>O 1.2, NaHCO<sub>3</sub> 25, glucose 11, ascorbic acid 0.4, sodium pyruvate 2(pH=7.4, 310 mOsm); 电极内液成份为(mmol/L): K-gluconate 130, KCl 5, EGTA 0.5, HEPES 10, Mg-ATP 4, Li-GTP 0.3, phosphocreatine di-

(tris) salt 10(pH=7.2, 300 mOsm); 河豚毒素(TTX)、氯化铯(CsCl)、ZD7288, 氯化镍(NiCl<sub>2</sub>)及米贝地尔(mibepradil)分别用去离子水配置成1000倍的母液,分装后-20 °C保存,实验当天用ACSF配置成终浓度。TTX购自Tocris, K-gluconate购自Wako,余试剂均购自Sigma。药物以重力的作用灌流至记录槽,药物之间的更换通过三方活栓进行。

### 1.3 全细胞膜片钳记录

参照我们之前的方法<sup>[8-9]</sup>,将孵育后的脊髓薄片移入记录槽(体积约为0.5 mL),以通有混合气的ACSF持续灌流,速度约2~4 mL/min。电生理记录在室温下(22~25 °C)进行。记录用玻璃微电极(TW150F-4, WPI)由电极拉制仪(P-97, Sutter)拉制而成,充灌电极内液后电极阻抗为3~5 MΩ。使用红外微分干涉相差显微镜(IR-DIC)对脊髓薄片进行观察(图1),SG区在低倍镜(×10)下呈半透明状,高倍镜(×40)下选取状态良好的SG神经元(胞体有立体感、轮廓清晰、表面光滑,常可见与胞体相连的较为完整的突起)进行记录,封接成功后电极阻抗可上升至2~5 GΩ。采用EPC-10膜片钳放大器进行电信号的放大,记录软件为Patchmaster。电压钳模式下测量SG神经元的膜电容和膜电阻,电流钳模式下测量静息电位、动作电位阈值、振幅和半宽度。参照以往的报道,纳入本研究中进行分析的神经元静息电位均较-40 mV更负<sup>[10]</sup>。

### 1.4 统计学分析

所有数据均以均数±标准误表示,n为神经元的数目,给药前后比较采用t检验进行分析,多组样本比较采用方差分析,P<0.05为差异具有统计学意义。

## 2 结果

### 2.1 脊髓背角SG神经元的基本电生理特性

如图1所示,脊髓背角SG区在低倍显微镜(BX51WI, Olympus)下为半透明区(图1A);高倍红外微分干涉相差镜(IR-1000, Dage-MIT)下可清晰的看到神经元形态(图1B),所有实验结果的记录均在全细胞膜片钳封接后5~10 min,电流稳定之后进行。本研究共对63个SG神经元进行了全细胞膜片钳记录,给予SG神经元时程1 s,大小为-120 pA的超极化刺激,可观察到细胞受超极化刺激(图1C紫色框内部分)后产生的去极化反应(图1C、D、E黑色箭头所指)。根据有或无去极化反跳及是否伴有放电,我们将SG神经元分为3组:无去极化反跳、有去极化反跳不伴放电和有去极化反跳伴放电,以下分别简称为无反跳(图1C)、反跳不伴放电(图1D)和反跳伴放电(图1E)。各组神经元的电生理学特点如表1所示:无反跳组和反跳伴放电组的动作电位阈值有显著差异(P<0.05),而各组的静息电位、膜电容、动作电位振幅和半宽度之间均无显著差异。

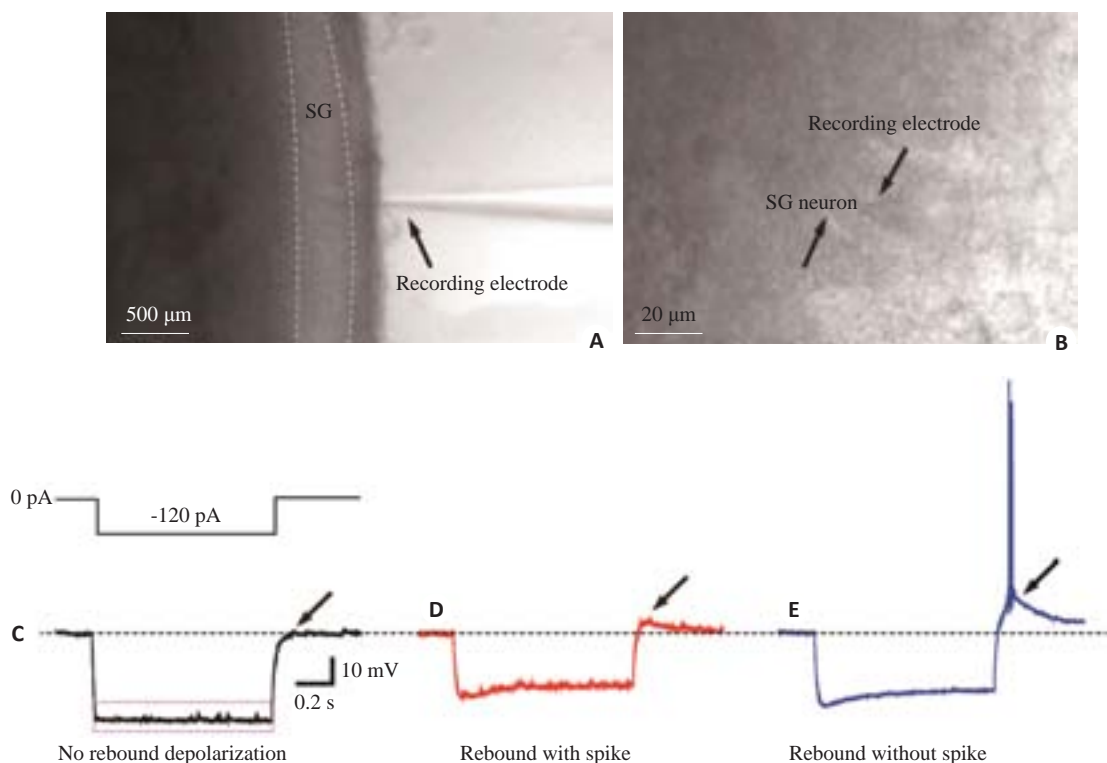


图1 脊髓背角SG神经元在显微镜下的形态及SG神经元接受超极化电流刺激后的代表性反应

Fig.1 Morphology and representative responses of SG neurons after hyperpolarization current stimulation. A, B: Representation of the position of SG in a parasagittal spinal cord slice (A) and IR-DIC image (B); C: No rebound depolarization; D: Rebound depolarization without spike; E: rebound depolarization with spike.

表1 SG神经元的基本电生理学特点

Tab.1 Electrophysiologic characteristics of SG neurons

Characteristics	Total	No rebound	Rebound without spike	Rebound with spike
n	63	23	19	21
RMP (mV)	-53.5±0.8	-55.3±1.6	-52.8±1.0	-52.1±1.5
C <sub>m</sub> (pF)	61.2±7.2	53.2±5.1	56.5±4.9	74.2±20.8
AP-T (mV)	-31.6±1.0	-28.7±1.6*	-30.3±1.0	-36.0±2.0*
AP-A (mV)	71.7±1.7	66.9±2.3	72.6±1.6	76.3±4.1
AP-HF (ms)	1.2±0.1	1.5±0.2	1.0±0.1	1.0±0.1

RMP: Resting membrane potential; C<sub>m</sub>: Membrane capacitance; AP-T: Threshold of action potential. AP-A: Amplitude of action potential; AP-HF: Half width of action potential. The action potential thresholds in no rebound depolarization group are significantly higher than those in rebound depolarization with spike group (\*P<0.05).

## 2.2 SG神经元去极化反跳的调控机制

为研究SG神经元去极化反跳的离子机制,我们分别测试了HCN通道阻断剂氯化铯和ZD7288,以及T型钙通道阻断剂氯化镍和米贝地尔对去极化反跳的作用。部分SG神经元在接受超极化刺激后产生去极化反跳(图2A),去极化反跳具有两个重要的参数:潜伏期和振幅,前者是指从超极化刺激结束到去极化反跳最高处的时间,后者是指静息电位与去极化反跳最高处的振幅差值(图2C)。为测量去极化反跳参数,我们在部分实

验中加入TTX(0.5 mol/L)以消除钠离子动作电位(图2B、图3B)。

ACSF中加入氯化铯(1 mmol/L)后(图2C,D),反跳伴放电的潜伏期从45.9±11.6 ms增加到121.6±51.3 ms(n=5,P<0.05),是用药前的2.57倍;而振幅变化不明显,用药前后的振幅分别为9.5±3.5 mV和9.8±3.4 mV(n=5,P>0.05)。部分研究认为,氯化铯是一种非选择性HCN通道阻断剂,为进一步验证HCN通道与反跳伴放电潜伏期的关系,我们观察了选择性HCN通道阻断剂ZD7288(0.01 mmol/L)的作用。与氯化铯的结果类似,ZD7288显著延长了反跳伴放电的潜伏期,从36.2±10.3 ms延长至73.6±13.6 ms(n=5,P<0.05),而对振幅无明显作用,用药前后的振幅分别为10.6±1.9 mV和10.5±1.3 mV(n=5,P>0.05,图2E,F)。此外,氯化铯和ZD7288显著减小了HCN通道电流(图2D,E,红色箭头)。

为观察T型钙通道的作用,我们在ACSF中加入氯化镍(0.2 mmol/L)(图3C,D),反跳伴放电的振幅从19.9±6.3 mV降到9.5±4.5 mV(n=4,P<0.05),是用药前的0.5倍;而潜伏期改变不明显,用药前后的潜伏期分别为41.8±15.4 mV和34.0±11.2 mV(n=4,P>0.05)。高选择性T型钙通道阻断剂米贝地尔(0.01 mmol/L)对反跳伴放电的作用与氯化镍类似,能显著降低振幅,从26.1±9.4 mV降到15.5±5.0 mV(n=4,P<0.05),而对潜伏期无明显影响,用药前后的潜伏期分别为37.2±4.6 mV和

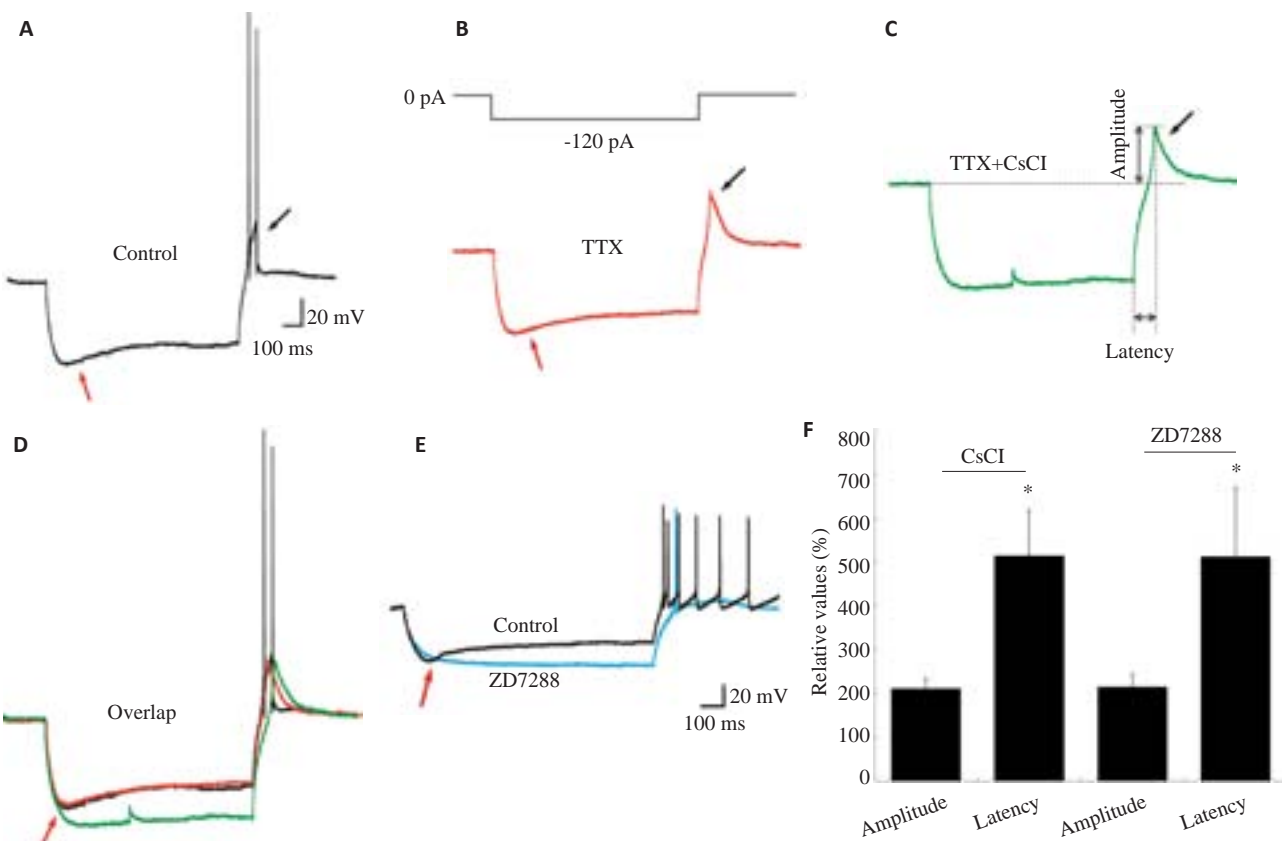


图2 HCN通道阻断剂对SG神经元去极化反跳伴放电的振幅和潜伏期的作用

Fig.2 Effects of HCN channel blockers on amplitude and latency of rebound depolarization with spike in SG neurons. **A**: Response of a SG neuron to -120 pA hyperpolarization current; **B**: Response of a SG neuron to TTX; **C**: Response of a SG neuron to TTX and CsCl; **D**: Superimposed traces of control, TTX, and CsCl shown in (A-C), which are from the same neuron; **E**: Rebound depolarization before and after ZD7288 treatment; **F**: CsCl and ZD7288 significantly delayed the latency of rebound depolarization with spike vs control (\* $P<0.05$ ) but had no effect on the amplitude ( $P>0.05$ ).

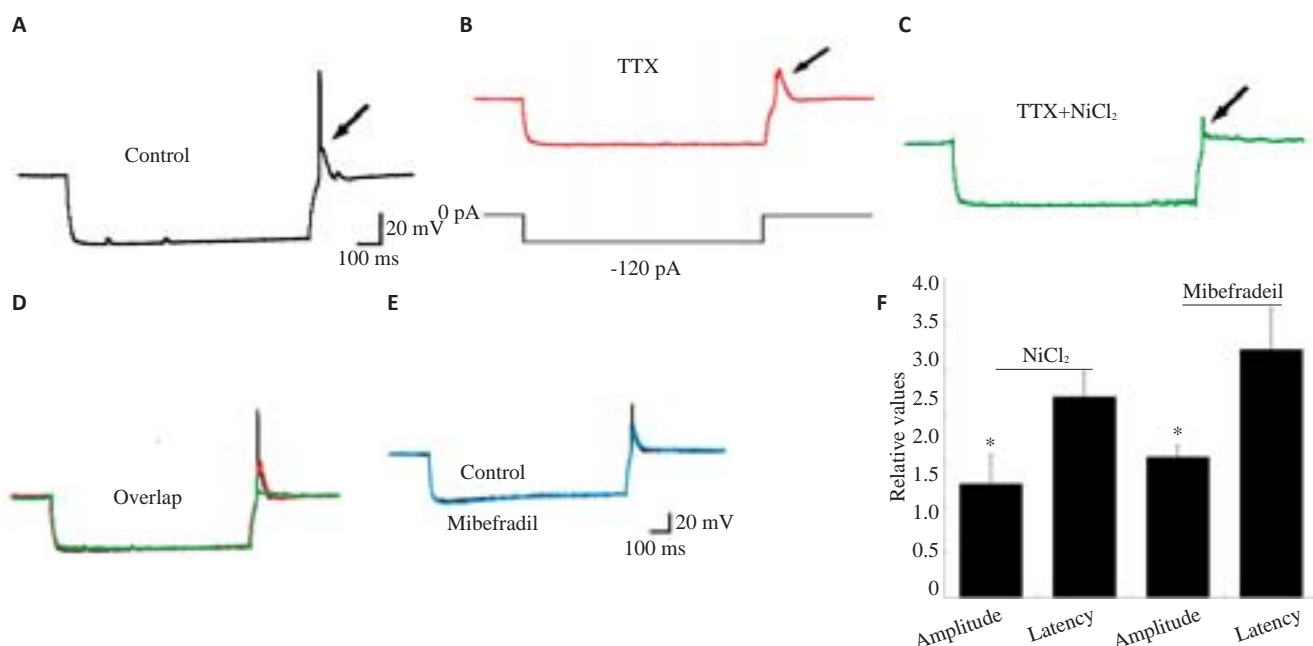


图3 T型钙通道阻断剂对SG神经元去极化反跳伴放电的振幅和潜伏期的作用

Fig.3 Effects of T-type calcium channel blockers on amplitude and latency of rebound depolarization with spike in SG neurons. **A**: Response of a SG neuron to -120 pA hyperpolarization current; **B**: Response of a SG neuron to TTX; **C**: Response of a SG neuron to TTX and NiCl<sub>2</sub>; **D**: Superimposed traces of control, TTX, and NiCl<sub>2</sub> shown in (A-C), which are from the same neuron; **E**: Rebound depolarization before and after mibepride treatment; **F**: NiCl<sub>2</sub> and mibepride significantly decreased the amplitude (\* $P<0.05$  vs control) but did not affect the latency of rebound depolarization with spike ( $P>0.05$  vs control).

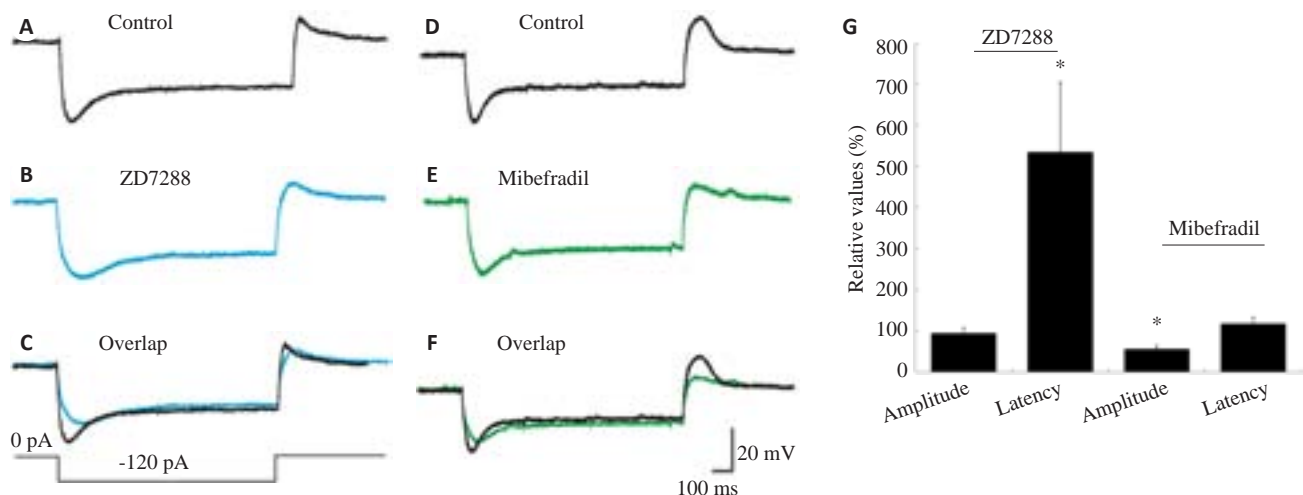


图4 HCN通道阻断剂和T型钙通道阻断剂对SG神经元去极化反跳不伴放电的振幅和潜伏期的作用

Fig.4 Effects of HCN channel and T-type calcium channel blockers on amplitude and latency of rebound depolarization without spike in SG neurons. A: Response of a SG neuron to -120 pA hyperpolarization current; B: Response of a SG neuron to ZD7288; C: Superimposed traces of control and ZD7288 shown in (A-B), which are from the same neuron; D: Response of a SG neuron to -120 pA hyperpolarization current; E: Response of a SG neuron to mibepradil; F: Superimposed traces of control and mibepradil shown in (D-E) which are from the same neuron; G: ZD7288 significantly delayed the latency (\*P<0.05 vs control) but did not affect the amplitude (P>0.05) of rebound depolarization without spike. Mibepradil significantly decreased the amplitude (\*P<0.05 vs control) but did not affect the latency (P>0.05) of rebound depolarization without spike.

41.2±8.2 mV( $n=4, P>0.05$ ,图3E,F)。

在反跳不伴放电的神经元中,ZD7288用药后的潜伏期从 $71.9\pm35.1$  ms增加到 $267.0\pm68.8$  ms( $n=5, P<0.05$ ),是用药前的5.34倍;而振幅变化不明显,用药前后的振幅分别为 $4.5\pm1.7$  mV和 $5.0\pm2.6$  mV( $n=5, P>0.05$ ),是用药前的0.94倍(图4B,C)。米贝地尔用药前后的潜伏期分别为 $43.1\pm9.6$  ms和 $46.2\pm6.6$  ms,用药后是用药前的1.17倍( $n=5, P>0.05$ );而振幅从 $14.3\pm3.0$  mV降低至 $7.9\pm2.0$  mV,是用药前的0.55倍( $n=5, P<0.05$ ,图4E,F)。与反跳伴放电组的结果类似,ZD7288显著延长了反跳不伴放电的潜伏期而对振幅无明显作用,米贝地尔能显著降低其振幅而对潜伏期无明显作用(图4G)。

以上结果表明,SG神经元的去极化反跳的潜伏期与HCN通道相关,振幅与T型钙通道相关。

### 3 讨论

去极化反跳可由内在神经环路的抑制性突触后电流(IPSC)或来自放大器的超极化电流刺激诱发,多见于具有自发性节律发放的神经元,如丘脑皮层神经元<sup>[1]</sup>,此外还见于无自发性节律发放的神经元,如海马CA1区椎体神经元<sup>[2]</sup>、内膝体神经元<sup>[3]</sup>和脊髓背角深层神经元<sup>[7]</sup>等。本研究发现约63%的脊髓背角SG神经元可记录到去极化反跳现象,其中53%的去极化反跳伴有动作电位的发放。

SG区神经元初步整合来自A8及C纤维传入的外周伤害性信息,这些信息再经过脊髓丘脑束等上行通路进入中枢神经系统高级部位,同时SG区还汇聚来自脑

干和大脑皮质的下行抑制性投射神经纤维,这些上行与下行系统连同局部的中间神经元共同构成了复杂的神经网络,是“闸门控制理论”的核心,尤其是该区域的长时程增强(LTP)在慢性疼痛的发生与发展中具有关键作用<sup>[13]</sup>。Yasaka等<sup>[10]</sup>发现成年SD大鼠中,具有去极化反跳的SG神经元约占所记录神经元的30%~40%,而在幼年C57BL/6小鼠的背角浅层神经元中,该比例不到30%<sup>[14]</sup>,均低于本研究中的比例。表明不同种属或脑区的神经元,不仅静息电位等基本内在电生理特性存在差异,超极化刺激诱发的去极化反跳也不完全相同。

动作电位阈值与神经元兴奋性有密切的关系,通常情况下,动作电位阈值越负,神经元兴奋性越高。本研究发现,反跳伴放电组比无反跳组神经元的动作电位阈值更负,提示前者与后者相比,在接受外来刺激信号时更容易兴奋,从而在整个神经回路中发挥调制作用。SG神经元按照末梢释放的递质不同,分为兴奋性和抑制性两大类<sup>[10]</sup>。“反跳伴放电”多见于抑制性中间神经元,表明其功能主要是接受下行抑制传入并将信息传递给其他神经元,维持局部神经网络的平衡。“反跳不伴放电”及“无反跳”在抑制性和兴奋性中间神经元中表达无明显差异<sup>[15-16]</sup>,为明确这两种现象在SG神经元中的功能需进行深入研究,如进行配对膜片钳或单细胞RT-PCR实验。

HCN通道和T型钙通道通过调控SG神经元去极化反跳的潜伏期和振幅,识别外周刺激强度及脊髓背角的抑制-兴奋信息间的转换,对整合躯体感觉信息具有重要的意义<sup>[7]</sup>。大量研究表明,去极化反跳的产生与T

型钙通道的去失活有关。静息状态下,电压依赖的T型钙通道处于失活状态,短暂的超极化刺激可解除T型钙通道的失活状态(此时仍为关闭状态),当撤去超极化刺激,细胞膜再次恢复到相对去极化的状态时,T型钙通道被激活<sup>[17]</sup>。T型钙通道的激活具有时间和电压依赖性,即超极化刺激强度越小,时间越长,诱发的T型钙通道的电流越小<sup>[5]</sup>。本研究的结果说明,SG神经元的去极化反跳的振幅受T型钙通道调控,阻断T型钙通道后,钙电流明显减少,导致振幅显著降低。T型钙通道有3种亚型:Cav3.1、Cav3.2和Cav3.3,基因敲除Cav3.1或基因沉默Cav3.2可显著减轻动物的痛敏。研究表明:T型钙通道与神经病理性疼痛相关,其阻断剂能减轻大鼠痛觉过敏<sup>[18-20]</sup>。在不同疼痛模型中的T型钙通道表达比例显著上升,阻断T型钙通道可有效缓解触诱发痛<sup>[21-22]</sup>。另外,SD大鼠坐骨神经结扎导致超极化激活的阳离子电流( $I_h$ )表达增加,而且在疼痛期间神经兴奋性增高,应用介导 $I_h$ 的HCN通道特异性阻断剂ZD7288后疼痛缓解<sup>[23-25]</sup>。以上研究表明HCN通道和T型钙通道在神经病理性痛的发生发展中具有重要的作用。本研究结果发现HCN通道和T型钙通道可调控脊髓背角SG神经元的去极化反跳的潜伏期和振幅,表明去极化反跳与慢性痛的发生机制密切相关。

本研究通过对急性分离脊髓切片的SG神经元进行全细胞膜片钳记录,探讨了表达去极化反跳的SG神经元的基本电生理特性,阐明了去极化反跳的离子机制,为临床治疗疼痛的药物研发提供了理论基础。

## 参考文献:

- [1] Todd AJ. Neuronal circuitry for pain processing in the dorsal Horn [J]. Nat Rev Neurosci, 2010, 11(12): 823-36.
- [2] Senatore A, Guan W, Spafford JD. Ca(v)3 T-type channels: regulators for gating, membrane expression, and cation selectivity [J]. Pflugers Arch, 2014, 466(4): 645-60.
- [3] Kopp-Scheinpflug C, Tozer AJ, Robinson SW, et al. The sound of silence: Ionic mechanisms encoding sound termination[J]. Neuron, 2011, 71(5): 911-25.
- [4] Aizenman CD, Linden DJ. Regulation of the rebound depolarization and spontaneous firing patterns of deep nuclear neurons in slices of rat cerebellum[J]. J Neurophysiol, 1999, 82(4): 1697-709.
- [5] Wang XX, Jin Y, Sun H, et al. Characterization of rebound depolarization in neurons of the rat medial geniculate body *in vitro* [J]. Neurosci Bull, 2016, 32(1): 16-26.
- [6] Ku WH, Schneider SP. Multiple T-type  $\text{Ca}^{2+}$  current subtypes in electrophysiologically characterized hamster dorsal Horn neurons: possible role in spinal sensory integration[J]. J Neurophysiol, 2011, 106(5): 2486-98.
- [7] Rivera-Arconada I, Lopez-Garcia JA. Characterisation of rebound depolarisation in mice deep dorsal Horn neurons *in vitro* [J]. Pflugers Arch, 2015, 467(9): 1985-96.
- [8] Liu NA, Zhang DY, Zhu MY, et al. Minocycline inhibits hyperpolarization-activated currents in rat substantia gelatinosa neurons[J]. Neuropharmacology, 2015, 95(8): 110-20.
- [9] 朱梦叶, 刘娜娜, 彭斯聪, 等. 米诺环素抑制大鼠脊髓背角胶质神经元的超极化激活电流[J]. 南方医科大学学报, 2015, 35(8): 1155-61.
- [10] Yasaka T, Tiong SY, Hughes DI, et al. Populations of inhibitory and excitatory interneurons in lamina II of the adult rat spinal dorsal Horn revealed by a combined electrophysiological and anatomical approach[J]. Pain, 2010, 151(2): 475-88.
- [11] Lee J, Song K, Lee K, et al. Sleep spindles are generated in the absence of T-type calcium channel-mediated low-threshold burst firing of thalamocortical neurons [J]. Proc Natl Acad Sci USA, 2013, 110(50): 20266-71.
- [12] Surges R, Sarvari M, Stevens M, et al. Characterization of rebound depolarization in hippocampal neurons [J]. Biochem Biophys Res Commun, 2006, 348(4): 1343-9.
- [13] 杨红卫, 张红梅, 胡晓东, 等. Pka参与脊髓背角c-纤维诱发电位ltp的诱导和早期维持[J]. 中国病理生理杂志, 2004, 20(4): 20-4.
- [14] Graham BA, Brichta AM, Schofield PR, et al. Altered potassium channel function in the superficial dorsal Horn of the spastic mouse [J]. J Physiol, 2007, 584(1): 121-36.
- [15] Lu Y, Perl ER. A specific inhibitory pathway between substantia gelatinosa neurons receiving direct C-fiber input [J]. J Neurosci, 2003, 23(25): 8752-8.
- [16] Lu Y, Perl ER. Modular organization of excitatory circuits between neurons of the spinal superficial dorsal Horn (laminae I and II) [J]. J Neurosci, 2005, 25(15): 3900-7.
- [17] Lambert RC, Bessah T, Crunelli VA. The many faces of T-type calcium channels[J]. Pflugers Arch, 2014, 466(3): 415-23.
- [18] Takasusuki T, Yaksh TL. Regulation of spinal substance p release by intrathecal Calcium Channel blockade[J]. Anesthesiology, 2011, 115(1): 153-64.
- [19] Leblanc BW, Lii TR, Huang JJ, et al. T-type calcium channel blocker Z944 restores cortical synchrony and thalamocortical connectivity in a rat model of neuropathic pain[J]. Pain, 2016, 157 (1): 255-63.
- [20] Bourinet E, Francois A, Laffray S. T-type calcium channels in neuropathic pain[J]. Pain, 2016, 157(2, 1): S15-22.
- [21] Sekiguchi F, Kawabata A. T-type calcium channels: functional regulation and implication in pain signaling [J]. J Pharmacol Sci, 2013, 122(4): 244-50.
- [22] Yue J, Liu L, Liu Z, et al. Upregulation of T-type  $\text{Ca}^{2+}$  channels in primary sensory neurons in spinal nerve injury[J]. Spine (Phila Pa 1976), 2013, 38(6): 463-70.
- [23] Du L, Wang SJ, Cui J, et al. The role of HCN channels within the periaqueductal gray in neuropathic pain[J]. Brain Res, 2013, 1500 (10): 36-44.
- [24] Zhang SZ, You Z, Wang SX, et al. Neuropeptide S modulates the amygdaloidal HCN activities ( $I_h$ ) in rats: Implication in chronic pain[J]. Neuropharmacology, 2016, 105(8): 420-33.
- [25] Smith T, Otaibi M, Sathish J, et al. Increased expression of hcn2 channel protein in l4 dorsal root ganglion neurons following axotomy of l5-and inflammation of l4-spinal nerves in rats [J]. Neuroscience, 2015, 295(7): 90-102.

(编辑:孙昌朋)